Indian Journal of Pure & Applied Physics
Vol. 57, December 2019, pp. 877-880

Selective and sensitive detection of CO gas by In_2O_3 thick film gas sensors

F K Ansari & M D Mahanubhav
Department of Physics, Z B Patil College, Dhule 424 002, India

Received 6 November 2018; accepted 21 August 2019

This study aims to provide a better fundamental understanding of the gas sensing mechanism of In_2O_3 gas sensors. In the present work In_2O_3 powder has been derived by calcinations of In_2S_3 powder prepared by flux method. Thick film of In_2O_3 has been deposited utilizing a relatively simple and low cost screen printing technique and characterized by scanning electron microscopy and X-ray diffraction. In_2O_3 thick film exhibits much higher sensitivity to CO at 150 °C. The corresponding sensitivity is 10.2 with good selectivity, and the response and recovery times are 6 and 14 s, respectively. The results indicate that the In_2O_3 thick film can be used to fabricate high performance CO sensors.

Keywords: Flux method, In_2O_3, Screen printing technique, CO, Sensors, Thick films

1 Introduction

Gas sensors have been exploited in recent years owning to their promises for improving our living standard in detecting toxic, explosive, harmful, colourless, odourless and combustible gases[1]. Interest in detecting gases and determining their composition has constantly been on the increase in recent years. Detection is important because it is necessary in many different fields. Most of the studies have focused on detecting CO_2, CO, SO_2, O_2, O_3, H_2, Ar, N_2, NH_3 and H_2O, because of their toxicity, their relation with atmospheric composition or the fact that they can be found at high levels in some environments[2]. Among them, carbon monoxide (CO) is a colourless, tasteless, and odour less gas that is notorious as an invisible silent killer. It is highly toxic, and it induces acute toxic symptoms such as headache, dizziness, weakness, irritability, confusion, depression, and an increase followed by a decrease in the pulse and respiratory rates[3]. Rabee *et al*. have been worked on highly sensitive photonic crystal fiber gas sensor and analysed it by full victoria finite element method. The reported gas sensor is a good and useful tool for detecting harmful gases[4]. Seekaew *et al.* investigated about a novel graphene-based electroluminescent gas sensor for the detection of CO_2. They showed a high selectivity of the sensor for carbon dioxide gas[5].

Indium oxide belong among transparent conducting oxides are widely used in various applications due to its low resistivity, high optical transparency and wide band gap[6]. In_2O_3 as a significant n-type semiconductor with a band gap (3.55-3.75 eV) has attracted intensive attention due to its special properties, such as low absorbance rate in the visible region, and high infrared light reflectivity[7]. Moreover, there is a growing interest in the synthesis of In_2O_3 nanostructures due to their controllable morphology with remarkable properties and potential applications in nanodevices[8].

Depending on the application, process temperature, thermal and chemical stability requirements, transparency and resistance become deciding factors in what material and by what method to adapt[9]. Flux method is effective for synthesis of high quality crystals, and the prepared crystals often have characteristic and uniformed shapes covered with particular flat facets. The crystallinity, the shape of the crystals or the particles is considered to be one of the key factors affecting the photocatalytic activity[10].

In this paper, we report a systematic investigation on the synthesis of In_2O_3 powder, properties of thick films of In_2O_3 deposited by screen printing technique, also sensitivity and selectivity against various gasses. The In_2O_3 thick film gas sensors exhibits excellent CO sensing properties at 150 °C.

2 Experimental Details

2.1 Synthesis of In_2O_3 powder

To synthesize the In_2O_3 powder, first In_2S_3 was prepared by flux method using sodium sulphide as a flux. AR grade powder of indium sulphate, sodium sulphide and sulphur were mixed in appropriate

*Corresponding author (E-mail: mahanubhav@rediffmail.com)

proportion so as to obtained stoichiometric In_2S_3 product. The mixture was ball milled for 2 h and then transferred into 50 ml crucible and heated into a muffle furnace. The temperature was increased to 600 °C with a heating rate of 60 °C/h. During heating excess sulphur get evaporated. The furnace was then switched off to allow it cool down to room temperature overnight. The product in crucible then washed several times with double distilled water. Sodium poly-sulphide got dissolved in water and separated out easily. Final product was dried.

It could be possible to derive oxides from the respective sulphides by calcinations at higher temperatures in air. Therefore, In_2S_3 was calcinated at 900 °C for 10 h in air in order to replace sulphur by oxygen so as to get the required In_2O_3 product.

2.2 Film formation

Screen printing technique was used for obtaining In_2O_3 thick films on glass substrates. Initially the In_2O_3 powder was thoroughly ground in an agate pestle mortar. The thixotropic paste was formulated by mixing the fine powder of In_2O_3 with solution of ethyl cellulose in a mixture of organic solvents such as butyl cellosolve, butyl carbitol acetate and terpineol. This paste was screen printed onto glass substrates. The wet films were dried under IR lamp and then fired at 200 °C for 30 min to remove organic binder.

2.3 Gas sensing

The sensing performance of the sensors was examined using a static gas sensing system. There were electrical feeds through the base plate. The heater was fixed on the base plate to heat the sample up to required operating temperature. A thermocouple was used to sense the temperature of the sensor. The output of the thermocouple was connected to a digital temperature indicator. A gas inlet valve was fitted at one of the posts of the base plate. The required gas concentration inside the static gas sensing system was achieved by injecting a known volume of a test gas using a gas injecting syringe. A constant voltage is applied to the sensor, and the current was measured by a digital picoammeter Model: DPM-111 (Scientific equipment Roorkee).

2.4 Characterization

The crystalline structure of the powder was analysed with Bruker X-ray diffractometer (D8, Advance, Brucker AXS Model) with Cukα radiation (λ = 1.5406 nm) radiation source in the 2θ range 10 - 80°. Scanning electron microscope Hitachi (S-4800, Hitachi, Japan) (SEM) was used to examine the surface morphology of films. Quantitative elemental analysis of the film was carried out by computer controlled energy dispersive X-ray analyser (EDAX) attached to the scanning electron microscope.

3 Results and Discussion

3.1 Elemental composition

The at % of In and O in In_2O_3 thick films were obtained by EDAX. The at % of In and O were found to be 41.03 and 58.97, respectively. For stoichiometric composition of In_2O_3, the theoretically expected at % of In and O are 40 and 60, respectively, from this it is clear that the results obtained by EDAX is matching well with theoretically expected stoichiometric composition of In_2O_3.

3.2 XRD analysis

Figure 1 shows XRD patterns of In_2O_3 thick films. The analysis of crystal structure revealed that the particles were found to be well identified as crystallized rhombohedral In_2O_3 [JCPDS - 01073-1809]. Different peaks in XRD pattern which appeared at 2θ values 30.970, 32.59, 37.642, 45.577, 50.171 and 60.541 were due to reflections from (104), (110), (113), (024), (116), (125) planes of In_2O_3, respectively. The peak intensity of the (113) plane was predominant among the other reflection planes indicating the preferential orientation of the In_2O_3 films. The presence of weak peaks revealed that In_2O_3 particles were partially crystalline in nature. The presence of vacant lattice site and local lattice disorder might lead to an obvious reduction or even disappearance in intensities of XRD peaks corresponding to lattice planes such as (110), (116) and

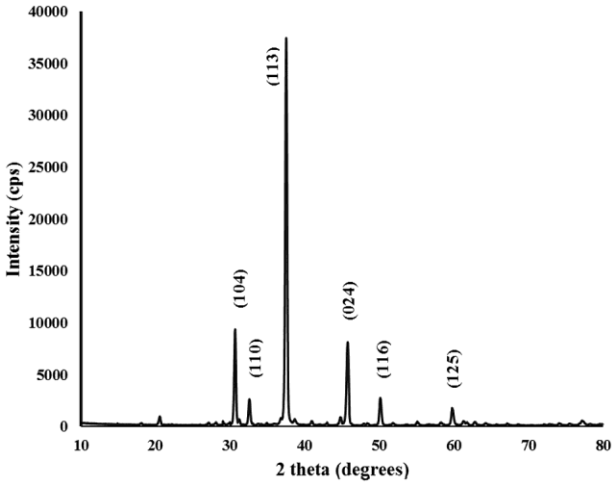

Fig. 1 – XRD patterns of In_2O_3 thick film.

(125). The disappearance and reduction in intensities of peaks from some of the lattice sites, refers to the destroyed periodicity and local lattice disorder, respectively. The average crystallite size was 319.3 nm.

3.3 Surface morphology

Figure 2(a) exhibits a typical SEM image of In_2O_3 thick film. High magnification SEM images are shown in Fig. 1(b and c). It is clear from figure that sample consisting of randomly distributed grains and all the surface of the film is highly rough as in Fig. 2(a). The roughness of the surface of a gas sensor can facilitate the enhanced sensitivity since high roughness is beneficial for more gas adsorption. It is evident that the surface area is drastically increased as to be favourable for gas to react.

3.4 Gas sensing performance

3.4.1 Sensing characteristics

Sensitivity (S) is the device characteristic of perceiving a variation in physical and chemical properties of sensing material under gas exposure. It is defined with following equation:

$$S = \frac{(G_g - G_a)}{G_a}$$

where, G_g and G_a are the conductance in the presence of test gas and in air, respectively.

3.4.2 Response of In_2O_3 thick film gas sensor

The selectivity is another key parameter for gas sensor, which is also crucial for practical application[11]. The response of the sensor to 1000 ppm of various testing gases at 150 °C is described in Fig. 3. In_2O_3 sensor shows an excellent selectivity to CO gas in comparison with H_2, SO_2, CO, Cl_2, H_2S, CO_2, and NH_3 gases. It is clear from the inset of figure that the response of the sensor to CO gas increases with increase in temperature ranging from 50 to 450 °C, attains its maximum and then decreases further with increase in temperature. The response to CO gas was observed to be highest (10.2) at 150 °C. The response and recovery time was 6 and 14 s, respectively.

Figure 4 shows the variation of sensitivity with respective gas concentration. From the figure one can conclude that the sensitivity increases with increasing gas concentration.

3.4.3 Sensing mechanism (reaction mechanism) of CO

The characteristic curve in the inset of Fig. 3 can be interpreted on the basis of adsorption-desorption and

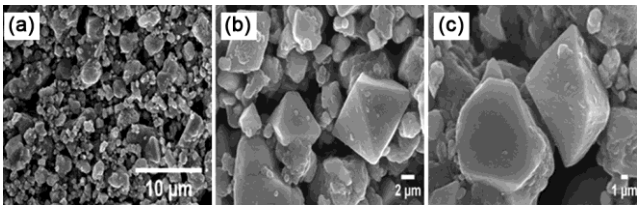

Fig. 2 – SEM micrograph of In_2O_3 thick film.

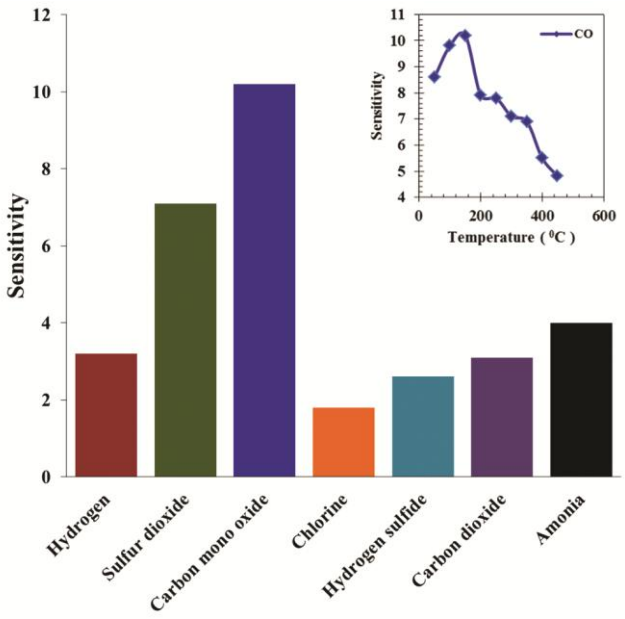

Fig. 3 – The selectivity of the In_2O_3 sensor to 1000 ppm for different gases at 150 °C. The inset is temperature-dependent sensitivity of the In_2O_3 sensor for CO gas.

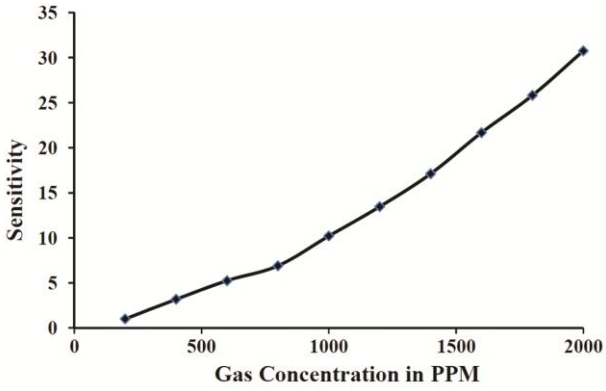

Fig. 4 – The variation of sensitivity with respective the gas concentration at 150 °C.

reaction process occurring on the sensing layer surface. At operating temperature < 100 °C the sensitivity is low because the adsorbed CO molecules are not activated enough to react with the surface adsorbed oxygen species. An increase in operating temperature above 100 °C contributes to overcome the activation

energy barrier to the reaction and significant increase in electron concentration results from the sensing reaction ($CO_{ads} + [O] \rightarrow CO_2 + \bar{e}$). However, above 150 °C the difficulty in CO gas adsorption is not adequately compensated by the increase of surface reaction and the sensitivity decreases.

4 Conclusions

The gas sensing properties of In_2O_3 thick films have been investigated. In_2O_3 powder could be obtained by calcinations of In_2S_3 prepared by flux method. Morphologies and microstructures of the sample were characterized by means of XRD and SEM. The gas sensing results shows that the response to CO gas was 10.2 at 150 ℃ in comparison with other gases tested.

Acknowledgment

One of the authors (F K Ansari**)** sincerely thanks to DST, Government of India for sanctioning INSPIRE fellowship (DST/INSPIRE Fellowship/2013/708).

References

1 Anand K, Kaur J, Singh R C & Thangraj R, *Ceram Int*, 42 (2016) 10957.
2 Cadena G J, Riu J & Rius F X, *Analyst*, 132 (2007) 1083.
3 Mirzaei A, Park S, Sun G J, Kheel H & Lee C, *J Hazard Mater*, 305 (2016) 130.
4 Rabee A S H & Obayya S S A, *Optik*, 188 (2019) 78.
5 Seekaew Y & Wongchoosuk C, *Appl Surf Sci*, 479 (2019) 525.
6 Hotovy I, Kups T, Hotovy J, Liday J, Bus D, Caplovicova M, Rehacek V, Sitter H, Simbrunner C, Bonanani A & Spiess L, *J Elect Eng*, 61 (2010) 382.
7 Liu J, Luo T, Meng F, Qian K, Wan Y & Liu J, *J Phys Chem C*, 114 (2010) 4887.
8 Abdullah Q N, Obaid A S & Bououdina M, *Ceram Int*, 44 (2018) 4699.
9 Cordonier C E J, Nakamura A, Yoshioka D, Shimada K & Fujishima A, *Thin Solid Films*, 534 (2013) 529.
10 Yamamoto A, Mizuba S, Saeki Y & Yoshida H, *Appl Catal A: Gen*, 521 (2016) 125.
11 Che Q , Ma S Y, Xu X L, Jiao H Y, Zhang G H , Liu L W, Wang P Y, Gengzang D J & Yao H H , *Sens Actuators B*, 264 (2018) 263.